



Mapping of spatial and temporal variation of water characteristics through satellite remote sensing in Lake Panguipulli, Chile

Pirjo Huovinen ^{a,b,*}, Jaime Ramírez ^a, Luciano Caputo ^a, Iván Gómez ^{a,b}

^a Instituto de Ciencias Marinas y Limnológicas, Universidad Austral de Chile, Valdivia, Chile

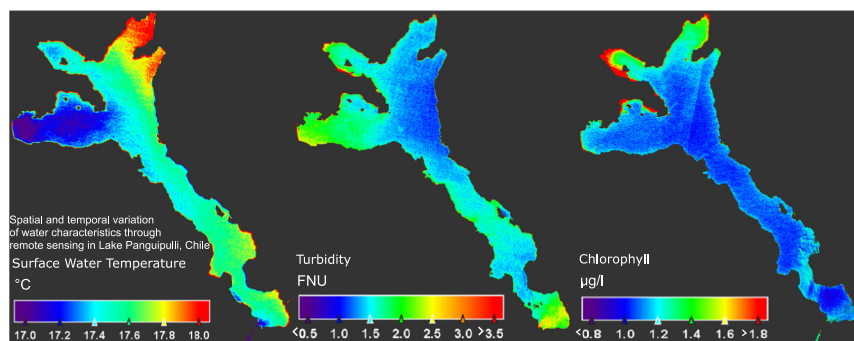
^b Centro FONDAP de Investigación en Dinámica de Ecosistemas Marinos de Altas Latitudes (IDEAL), Valdivia, Chile



HIGHLIGHTS

- Large Chilean Lake Panguipulli was studied through remote sensing.
- Surface water temperature, turbidity and chlorophyll *a* showed intra-lake variation.
- Satellite data allowed wider observational scales of seasonal and spatial anomalies.
- Mapping provided detailed synopsis of sensitive areas for monitoring programs.

GRAPHICAL ABSTRACT



ARTICLE INFO

Article history:

Received 21 February 2019

Received in revised form 24 April 2019

Accepted 25 April 2019

Available online 1 May 2019

Editor: Damia Barcelo

Keywords:

Chlorophyll

Landsat 5/7/8

Large lake

Sentinel-2

Temperature

Turbidity

ABSTRACT

Central-southern Chile is characterized by a series of large lakes that originate in the Andes Mountains. This region is facing increasing anthropogenic impact, which threatens the oligotrophic status of these lakes. While monitoring programs are often based on a limited spatial and temporal coverage, remote sensing offers promising tools for large-scale observations improving our capacity to study comprehensively indicators of lake properties. Seasonal trends (long-term means) and intra-lake variation of surface water temperature (SWT), turbidity and chlorophyll *a* in Lake Panguipulli were studied through satellite imagery from Landsat 5 TM, 7 ETM+ and 8 OLI (1998–2018; SWT, turbidity), and Sentinel-2A/B MSI (2016–2017; chlorophyll). Remotely sensed data were validated against *in situ* data from monitoring database. Satellite-derived SWT (representing the surface skin layer of water, so-called skin temperature) showed good similarity with *in situ* (bulk) temperature (RRMSD 0.17, $R^2 = 0.86$), although was somewhat lower (RMSD of 2.77 °C; MBD of –2.10 °C). Seasonal long-term means of turbidity from satellite imagery corresponded to those from *in situ* data, while satellite-derived predictions (based on OC2v2 algorithm) overestimated chlorophyll *a* levels slightly in summer–spring. SWT ranged from 8.0 °C in winter to 17.5 °C in summer. Mean turbidity (1.6 FNU) and chlorophyll *a* (1.1 µg L⁻¹) levels were at their lowest in summer. Spatial and seasonal patterns reflected the bathymetry and previously described mixing patterns of this monomictic lake: warming of shallow bays in spring extended to wider area along with summer stratification period, while mixing of the water column was reflected in spatially more homogenous SWT in fall–winter. Spatial heterogeneity in summer was confirmed by a clear separation of different lake areas based on SWT, turbidity and chlorophyll *a* using 3-D plot. Mapping of spatial and seasonal variation using satellite imagery allowed identifying lake areas with different characteristics, improving strategies for water resource management.

© 2019 Elsevier B.V. All rights reserved.

* Corresponding author at: Instituto de Ciencias Marinas y Limnológicas, Universidad Austral de Chile, Valdivia, Chile.

E-mail address: pirjo.huovinen@uach.cl (P. Huovinen).

1. Introduction

Central-southern Chile is characterized by a series of large pre-mountain lakes (so-called North Patagonian lakes) originating in the Andes Mountains. They have been described as monomictic, temperate lakes, with highly transparent, oligotrophic waters (Campos et al., 1981; Soto, 2002). The very low chlorophyll *a* levels that are maintained in these lakes have been explained by nitrogen limitation and deep mixing depth (Soto, 2002), although the role of phosphorus was not ruled out (Steinhart et al., 2002). Nitrogen limitation, commonly observed in freshwater ecosystems of this region, has been associated with the high capacity of the surrounding native forest soils to retain inorganic nitrogen (Perakis and Hedin, 2002; Huygens et al., 2008) and with the low deposition of atmospheric nitrogen (in contrast to polluted regions in the northern hemisphere) (Hedin et al., 1995; Perakis and Hedin, 2002). Based on a recent analysis of a long-term monitoring database, increase of nutrients and decrease of temperature at deeper layers

was observed in ten lakes of this region over an 18-year period (1990–2008). The observed deep-water cooling trend was linked with enhanced melting of glaciers, while deforestation and expansion of urban areas was associated with the elevated nutrient input (Pizarro et al., 2016). In fact, this region is currently facing multiple environmental threats ranging from changes in land-use patterns and intensive anthropogenic intervention (e.g. fish farming, urbanization, tourism) (Pizarro et al., 2010; Echeverría et al., 2012; León-Muñoz et al., 2013) and global change, which has been evidenced by enhanced melting of glaciers (Bown and Rivera, 2007) and changes in the regimes of temperature (Pizarro et al., 2016) and precipitations (Boisier et al., 2016). As these lakes present contrasting characteristics to temperate lakes of the northern hemisphere (Baigún and Marinone, 1995; Perakis and Hedin, 2002; Steinhart et al., 2002; Llames and Zagarese, 2009), their responses to environmental changes cannot be predicted based on observed processes in lakes from other geographical locations.

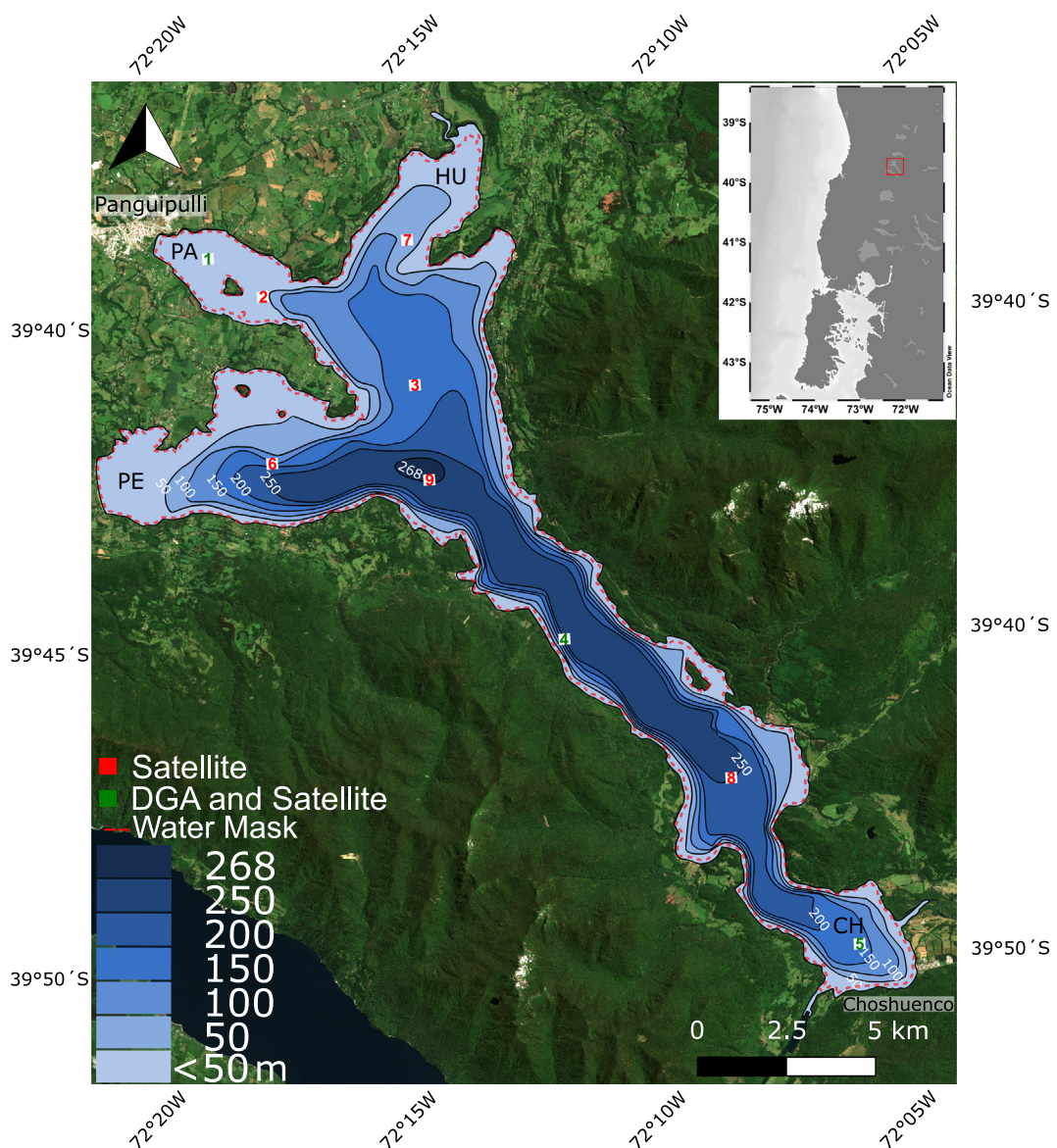


Fig. 1. Lake Panguipulli in central-southern Chile (geographical location indicated with red square in the inset figure). Three sites (1, 4, 5; green numbers) of *in situ* measurements (data from the database of Red Mínima de Lagos of Dirección General de Aguas, DGA, Ministry of Public Works, Chile) were used for ground validation. 10×10 pixel areas (white box) are indicated for nine sites (1–9; red and green numbers) used for specific satellite data analyses (in addition to analyses of all the pixels covering the whole lake area). Bathymetric map is redrawn from Campos et al. (1981) on Sentinel-2 image. Water body mask is also indicated. PA = Panguipulli Bay; PE = Peligro Bay; HU = Huanehue Bay; CH = Choshuenco Bay. Ocean Data View (Schlitzer, R. 2016, <http://odv.awi.de>) used in map creation.

Table 1

The used Sentinel-2A/B and Landsat 5/7/8 images for the four seasons and the analysed parameters.

| Season | Satellite | Date | Parameter | | | Season | Satellite | Date | Parameter | | |
|--------|-----------|----------|-----------|-----------|-----|--------|-----------|----------|-----------|-----------|-----|
| | | | SWT | Turbidity | Chl | | | | SWT | Turbidity | Chl |
| Summer | L5 | 14-02-98 | x | x | | Winter | L7 | 21-09-99 | | x | |
| | L7 | 11-01-00 | x | x | | | L5 | 10-09-04 | x | x | |
| | L7 | 27-01-00 | x | | | | L5 | 13-09-05 | x | x | |
| | L7 | 01-02-02 | x | | | | L5 | 14-07-06 | x | x | |
| | L7 | 03-01-03 | x | x | | | L5 | 30-07-06 | x | x | |
| | L7 | 20-02-03 | x | x | | | L5 | 18-08-07 | x | x | |
| | L7 | 24-03-03 | x | x | | | L7 | 17-07-10 | x | x | |
| | L5 | 14-01-04 | x | x | | | L7 | 02-08-10 | x | | |
| | L5 | 16-01-05 | x | x | | | L7 | 21-08-11 | x | x | |
| | L5 | 05-03-05 | x | x | | | L7 | 22-09-11 | x | x | |
| | L5 | 21-03-05 | x | x | | | L7 | 08-09-12 | x | x | |
| | L5 | 20-02-06 | x | | | | S2A | 01-09-16 | | | x |
| | L5 | 06-01-07 | x | x | | | S2A | 25-07-17 | | | x |
| | L5 | 23-02-07 | x | x | | | S2A | 16-09-17 | | | x |
| | L5 | 10-02-08 | x | x | | Spring | L5 | 29-11-98 | x | x | |
| | L5 | 26-02-08 | x | x | | | L7 | 23-10-99 | | | |
| | L5 | 12-02-09 | x | x | | | L7 | 10-12-99 | x | x | |
| | L5 | 28-02-09 | x | | | | L7 | 29-11-01 | x | x | |
| | L5 | 19-03-10 | | x | | | L5 | 23-12-01 | x | x | |
| | L7 | 27-03-10 | x | x | | | L7 | 02-10-03 | x | x | |
| | L7 | 09-01-11 | x | x | | | L5 | 10-10-03 | x | x | |
| | L5 | 18-02-11 | | x | | | L5 | 27-11-03 | x | x | |
| | L7 | 26-02-11 | x | | | | L5 | 12-10-04 | x | x | |
| | L7 | 12-01-12 | x | x | | | L5 | 19-11-06 | x | x | |
| | L7 | 14-01-13 | x | x | | | L5 | 05-12-06 | x | x | |
| | L7 | 03-03-13 | x | | | | L5 | 24-11-08 | | | |
| | L8 | 26-02-14 | x | x | | | L5 | 10-12-08 | x | x | |
| | L8 | 28-01-15 | x | x | | | L7 | 05-10-10 | x | x | |
| | S2A | 05-03-16 | | x | | | L7 | 27-12-11 | x | | |
| | L8 | 19-03-16 | x | x | | | L7 | 10-10-12 | x | | |
| | L8 | 01-01-17 | x | x | | | L7 | 11-11-12 | x | x | |
| Fall | S2A | 05-02-17 | | x | | | L7 | 27-11-12 | x | x | |
| | L8 | 06-03-17 | x | x | | | L8 | 24-12-13 | x | | |
| | L8 | 05-02-18 | x | x | | | L8 | 24-10-14 | x | x | |
| | L5 | 03-04-98 | x | x | | | L8 | 11-12-14 | x | | |
| | L7 | 16-04-00 | x | x | | | L8 | 11-10-15 | x | | |
| | L7 | 01-05-11 | x | x | | | L8 | 28-11-15 | x | | |
| | L7 | 06-05-13 | | x | | | S2A | 17-11-16 | | | x |
| | L7 | 07-06-13 | x | x | | | L8, S2A | 30-11-16 | x | | |
| | L8 | 18-06-14 | x | x | | | S2A | 27-12-16 | | | x |
| | L8 | 06-05-16 | | x | | | S2B | 27-11-17 | | | x |
| | S2A | 29-04-17 | | x | | | S2B | 17-12-17 | | | x |
| | L8 | 09-05-17 | x | | | | | | | | |
| | S2A | 19-05-17 | | x | | | | | | | |

Overall lakes can be regarded as good sentinels of environmental change owing to their relative sensitivity, rapid responses, and as they reflect and incorporate changes also from their wider catchment area and atmosphere (Adrian et al., 2009; Williamson et al., 2008, 2009a, 2009b). Currently the role of lakes as hot spots of carbon cycling and regulators of climate has been recognized (Williamson et al., 2009b). Along with the growing awareness regarding the importance of lakes, not only in regional but also in a global scale context, there is an urgent need to gain better understanding on their status and processes (Shimoda et al., 2011; Palmer et al., 2015). A recent special issue has also drawn attention to the Patagonian lakes as sensors of global change (Modenutti and Balseiro, 2018).

Lake Panguipulli is one of the large lakes in the north Patagonian lake district in Chile (Fig. 1). It is situated in the Valdivian temperate forest eco-region, which is among the 25 areas identified as biodiversity hotspots based on high endemism of species together with exceptional loss of habitat (Myers et al., 2000). Within this eco-region, UNESCO declared in 2007 a Biosphere Reserve with unique and globally important biodiversity (Pino et al., 2014). Limnological description of this lake in the mid 1970s by Campos et al. (1981) revealed maximum transparency (Secchi depth around 15 m) in summer, while in winter-spring the water clarity decreased markedly (around 5 m). The higher nitrate levels in winter coincide with the maximal chlorophyll *a* levels reported

Table 2

Characteristics of the Sentinel-2A/B and Landsat 5/7/8 bands that were used for the index calculations. In the case of the bands 11 and 12 of Sentinel with lower resolution, the pixels were transformed to 10 m pixels by resampling (ACOLITE, SNAP).

| Band | Waveband (nm) | Pixel (m) | Characteristics |
|---------------|---------------|-----------|-----------------|
| Sentinel-2A/B | | | |
| 2 | 440–538 | 10 | Blue |
| 3 | 537–582 | 10 | Green |
| 8 | 760–908 | 10 | NIR |
| 11 | 1539–1682 | 20 | Swir1 |
| 12 | 2078–2320 | 20 | Swir2 |
| Landsat-5/7 | | | |
| 2 | 520–600 | 30 | Green |
| 3 | 630–690 | 30 | Red |
| 4 | 770–900 | 30 | NIR |
| 5 | 1500–1750 | 30 | Swir1 |
| 6 | 10,400–12,500 | 30 | Thermal band |
| 7 | 2090–2350 | 30 | Swir2 |
| Landsat-8 | | | |
| 3 | 533–590 | 30 | Green |
| 4 | 636–673 | 30 | Red |
| 5 | 851–879 | 30 | NIR |
| 6 | 1566–1651 | 30 | Swir1 |
| 7 | 2107–2294 | 30 | Swir2 |
| 10 | 10,600–11,190 | 30 | Thermal band 1 |
| 11 | 11,500–12,510 | 30 | Thermal band 2 |

Table 3

Algorithms and satellite bands used to calculate Automated Water Extraction Index (AWEI), sensor brightness temperature, turbidity and chlorophyll *a*, and the software used for their analysis.

| Parameter | Algorithm | Satellites and bands | | | Software |
|-----------------|---|----------------------|-------------|------------|---------------|
| | | Sentinel-2 | Landsat 5/7 | Landsat 8 | |
| Water body mask | AWEI ^a | 3, 8, 11, 12 | 2, 4, 5, 7 | 3, 5, 6, 7 | SNAP |
| Temperature | Top-of atmosphere brightness temperature ^b | – | 6 | 10, 11 | ACOLITE, SNAP |
| Turbidity | T_Dogliotti ^c | – | 3, 4 | 5, 4 | ACOLITE |
| Chlorophyll | CHL_OCv2 ^d | 2, 3 | – | – | ACOLITE |

^a Feyisa et al., 2014.

^b <https://landsat.usgs.gov/landsat-8-l8-data-users-handbook-section-5>.

^c Dogliotti et al., 2015.

^d O'Reilly et al., 2000; https://oceancolor.gsfc.nasa.gov/atbd/chlor_a/.

for that season (Campos et al., 1981; Pizarro et al., 2016). Despite the observed tendencies in long-term water properties, Lake Panguipulli has maintained an overall oligotrophic status (Pizarro et al., 2016). However, many of its current environmental classifications are based on data with a very limited spatial and temporal coverage. Access to free satellite data in recent years has opened new possibilities to use remote sensing as a complementary tool in environmental monitoring, improving substantially the observational (spatial and temporal) scales (reviewed by Palmer et al., 2015; Dörnhöfer and Oppelt, 2016). In conjunction with traditional monitoring programs it can provide more comprehensive data for watershed management (Schaeffer et al., 2013). Remote sensing has proved to be a useful tool in water resource management (Giardino et al., 2010, 2014), supporting definition of water quality status (Bresciani et al., 2012, 2018) and monitoring programs (Philipson et al., 2016; Toming et al., 2016), however, has been mainly applied in the watersheds of the northern hemisphere (Dörnhöfer and Oppelt, 2016).

In the present study, remote sensing techniques were applied to estimate the water quality status of Lake Panguipulli using key parameters (surface water temperature (SWT), turbidity and chlorophyll *a*) that could be predicted through satellite imagery and validated through field observations. The aim was to 1) validate the satellite derived data against *in situ* data from monitoring database, and 2) use remote sensing to evaluate seasonal patterns and 3) intra-lake variation of water characteristics in Lake Panguipulli. In order to present representative overall mean seasonal trends, satellite imagery from 1998 to 2018 (Landsat 5/7/8; SWT and turbidity) and 2016–2017 (Sentinel-2; chlorophyll) were analysed. Mapping of seasonal and spatial variation of inherent water properties will give insights into the intra-lake heterogeneity, allowing identifying zones with higher susceptibility to environmental changes and thus improving strategies for water resource management and planning of monitoring programs.

2. Materials and methods

2.1. Study area

Lake Panguipulli ($39^{\circ} 43' S$, $72^{\circ} 13' W$) is considered a warm monomictic lake, with summer stratification (surface temperature 21 °C, hypolimnion 9 °C, thermocline reaching 40 m depth towards fall) and circulation in winter (homothermia 9 °C in August) (Campos et al., 1981). This fjord type lake with glacial origin is situated in a deep Tertiary valley basin, which presents a deep, narrow canal that widens towards west dividing into shallower bays (Fig. 1). The maximum depth of the lake is 268 m, the mean depth is 126 m, while approximately 23% of the lake has a depth of <30 m. The lake is 28 km long, 9.7 km wide at its maximum, and has a surface area of 117 km² and catchment area of 3811 km² (Campos et al., 1981). It receives water mainly from Llanquihue and Huanehue Rivers (both connected to other lakes), in addition to five other smaller tributaries. The only outflow is through the Enco River. Campos et al. (1981) estimated a theoretical renewal time of 16 months.

The main land use practices within the basin area are native forests (84%) and livestock pasture (15%). Wetlands comprise 1.2% of the basin area, while urban and open areas and forest plantation are less represented (0.01–0.03% each) (Pizarro et al., 2016). The main populated areas are town Panguipulli (around 34.500 inhabitants) and Choshuenco (<1000 inhabitants). Some of the rivers have fish aquaculture activities. Mean annual precipitation in this region (with rainy temperate climate) varies between 1800 and 2900 mm (Pizarro et al., 2016). Precipitation is highest in winter, snowing occurring above approximately >800 m altitude (Steinhart et al., 2002). In this region, there are active volcanoes, e.g. Villarrica, Llaima and Lonquimay (SERNAGEOMIN, <https://www.sernageomin.cl/red-nacional-de-vigilancia-volcanica/>).

2.2. Satellite imagery

Satellite images of Lake Panguipulli (Fig. 1) presenting clear sky conditions for the major part of the lake area were selected, covering a period from 1998 to 2018 for Landsat 5/7/8 and 2016–2017 for Sentinel-2

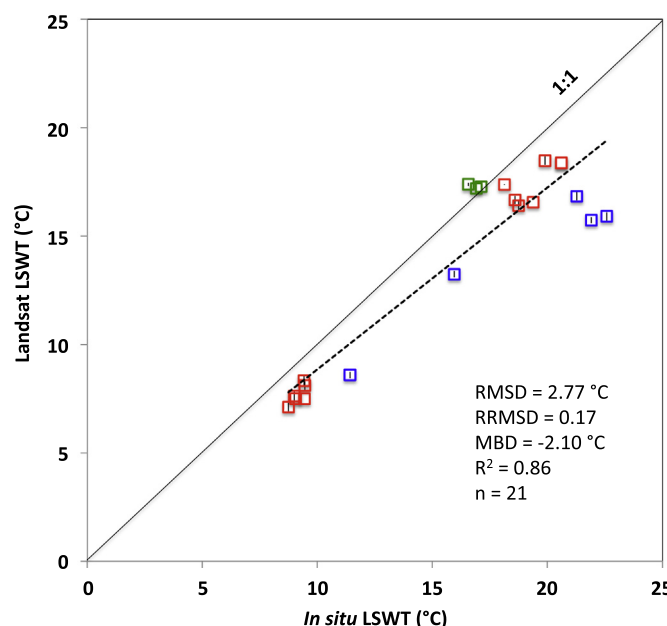


Fig. 2. Validation of the satellite (Landsat 5 (red), Landsat 7 (blue) and Landsat 8 (green)) derived surface water temperature (SWT; skin temperature) of Lake Panguipulli with *in situ* measurements (bulk temperature) obtained from the database of Red Mínima de Lagos of Dirección General de Aguas (DGA, Ministry of Public Works, Chile; 2006–2012) and additional measurements (2016). Root mean square difference (RMSD), root mean square relative difference (RRMSD), mean bias difference (MBD) and linear regression (dashed line; R^2) of also given. The satellite data used for validation correspond to 3 × 3 pixel area around three sampling sites 1, 4 and 5 (see Fig. 1).

(A, B) (see Table 1 for dates for the images). Images of surface reflectance from Landsat 5 Thematic Mapper (TM), Landsat 7 Enhanced Thematic Mapper Plus (ETM+), Landsat 8 Operational Land Imager (OLI) and Sentinel-2 (A, B) MultiSpectral Instrument (MSI) were used, all obtained from the free access page (<https://earthexplorer.usgs.gov/>). Map projection was WSG 84/UTM zone 18s, time of all satellites around 14:30 UTC. Variation of the zenith angle was from 31° (end of December) to 71° (end of June).

Landsat images were processed with ACOLITE software (Windows version 20180419.0), which is optimized for sea and freshwater using SWIR parameters for atmospheric correction (Vanhellemont and Ruddick, 2015). To mask clouds, cirrus and shadows, the Quality Assessment (QA) bands were used and confirmed with visual inspection. Atmospheric correction for Sentinel-2 images was carried out through the Sen2cor module of the Sentinel Application Platform (SNAP version 6.0) software, provided by the European Space Agency (ESA) in the STEP platform (<http://step.esa.int/main/>). The masks provided by Sen2cor level-2A algorithm Scene Classification (SCL masks) were used for clouds and shadows (see Huovinen et al., 2018). The gaps in the images of Landsat 7 from 2003 onwards, due to the failure of the scan line corrector (SCL), were filled with the SCL-off gap mask files using the program Qgis 2.14. The obtained Rayleigh-corrected reflectance (R_{rc}) data was used to calculate Automated Water Extraction Index (AWEI; Feyisa et al., 2014; Tables 2–3) manually with SNAP in order to separate the lake area from terrestrial environments (water body mask).

Within the water area (AWEI mask), temperature of Landsat 8 images, indices for turbidity and chlorophyll *a* were analysed directly with ACOLITE (Tables 2–3). For turbidity (FNU), a single-band, switching algorithm of Dogliotti et al. (2015) (T_Dogliotti), using red band at reflectance (red) <0.05, NIR band for reflectance (red) >0.07 and linear weighting in the transition zone (0.05–0.07), was applied. For chlorophyll *a*, the Ocean Chlorophyll two-band (OC2v2) algorithm based on blue/green band ratio (based on O'Reilly et al., 1998; updated by O'Reilly et al., 2000) was used. This algorithm was not suitable for Landsat (data not shown) thus Sentinel-2 with shorter-term data was used. Temperature of Landsat 5/7 images was processed using SNAP software, first transforming the digital numbers to radiance and then to top-of-atmosphere brightness temperature (<https://landsat.usgs.gov/landsat-8-l8-data-users-handbook-section-5>) (Tables 2–3). Infrared sensors measure thermal emission from the surface skin layer of water (so-called skin temperature) in contrast to *in situ* measurements below surface reaching a deeper water layer (bulk temperature).

Further processing of all the indices and data was carried out with SNAP software. Summer (January–March), fall (April–June), winter (July–September) and spring (October–December) means were calculated for each pixel (spatial variation) as well as for the whole lake area using available images from the 1998–2018 (Landsat) or 2016–2017 (Sentinel) period. Due to the climatic conditions and zenith angle, the amount of suitable images for analyses was lower for fall and winter (Table 1). For nine selected sites (see Fig. 1), 3 × 3 pixel area (for temperature) or 10 × 10 pixel area (for turbidity and chlorophyll due to higher heterogeneity of these parameters and smaller pixel size of Sentinel-2 used for chlorophyll) was used to calculate monthly means, and were also used for comparison with *in situ* measurements (see below). Site 4 is closest to the shore (360 m measured from the center of pixel). Sites 1 and 7 are 750–800 m from the shoreline, while sites 2, 5, 8 and 9 are within 1–1.4 km range. Sites 3 and 6 are the most pelagic (1.6–1.8 km from the shore) (Fig. 1).

2.3. Field verification

Near-surface water data on temperature, turbidity and chlorophyll *a* obtained from the monitoring database of the National Network of Minimum Lake Control (Red Nacional Mínima de Control de Lagos) of the General Water Directorate (Dirección General de Aguas,

DGA) of the Ministry of Public Works of Chile (<http://www.dga.cl/servicioshidrometeorologicos/>) were used for field verification. *In situ* data from three sampling sites (see Fig. 1) for Lake Panguipulli were available for a period of 2000–2012. Chlorophyll *a* was analysed spectrophotometrically from filtered samples (Jeffrey et al., 1997), while temperature and turbidity were measured *in situ* with multiparameter sonde (DGA, 2007; values >0 FNU were used). Additional near-surface temperature measurements were made in the same sampling sites in November 2016. The satellite data correspond to 3 × 3 (temperature) or 10 × 10 (turbidity and chlorophyll) pixel area around the three DGA sampling sites (1, 4, 5; see Fig. 1). In addition, sites 2 and 3 (currently site of DGA) were included in the chlorophyll analyses in order to increase the number of observations. Landsat 5/7/8 images of 1998–2018 (for temperature and turbidity) and Sentinel-2A/B images of 2016–2017 (for chlorophyll) were processed.

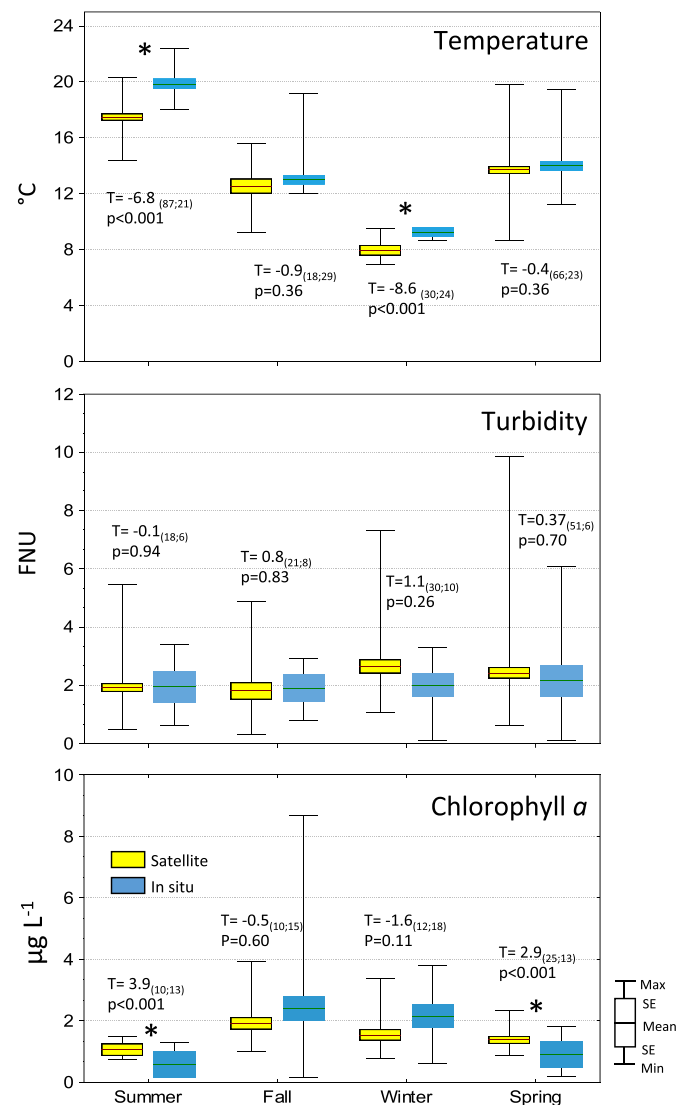


Fig. 3. Comparison between satellite derived and *in situ* data (mean \pm SE (min–max), n given in parenthesis inside the figure) on surface water temperature, turbidity and chlorophyll *a* in Lake Panguipulli within each season (* significant differences according to *t*-test). *In situ* data from 2000 to 2012 was obtained from the database of Red Mínima de Lagos of Dirección General de Aguas (DGA, Ministry of Public Works, Chile). The satellite data correspond to 3 × 3 (temperature) or 10 × 10 (turbidity and chlorophyll) pixel area around the three DGA sampling sites (1, 4, 5; for chlorophyll also sites 2 and 3 were included; see Fig. 1). Landsat 5/7/8 images of 1998–2018 (for temperature and turbidity) and Sentinel-2A/B images of 2016–2017 (for chlorophyll) were used. Statistical analyses of seasonal differences for the satellite data are given in Table 4.

Linear regression between satellite derived SWT (skin temperature) and *in situ* SWT (bulk temperature), as well as root mean square difference (RMSD), root mean square relative difference (RRMSD) and mean bias difference (MBD) were analysed. Due to that coincidence of dates between field monitoring dates and available satellite images was limited, match-up window of 0–6 days (with one exception of 9 days) for satellite and *in situ* data were used. In the case of turbidity and chlorophyll *a*, due to the lack of match-up of the dates, differences between satellite-derived and *in situ* data within each season were tested using *t*-test. Seasonal differences of remotely sensed data were compared using one-way ANOVA followed by Tukey post-hoc test ($p > 0.05$).

3. Results

3.1. Validation of satellite data

Landsat 5/7/8 derived SWT (skin temperature) showed linear correlation with *in situ* SWT (bulk temperature) ($R^2 = 0.86$), RRMSD (0.17) also confirming a relatively good similarity between satellite and field data. However, overall predicted SWT from satellite imagery was lower than observed SWT, with RMSD of $2.77\text{ }^\circ\text{C}$ and MBD of $-2.10\text{ }^\circ\text{C}$ (Fig. 2).

When comparing seasonal means of long-term data sets, in winter and summer satellite SWT was $1.3\text{--}2.3\text{ }^\circ\text{C}$ lower than field data, while

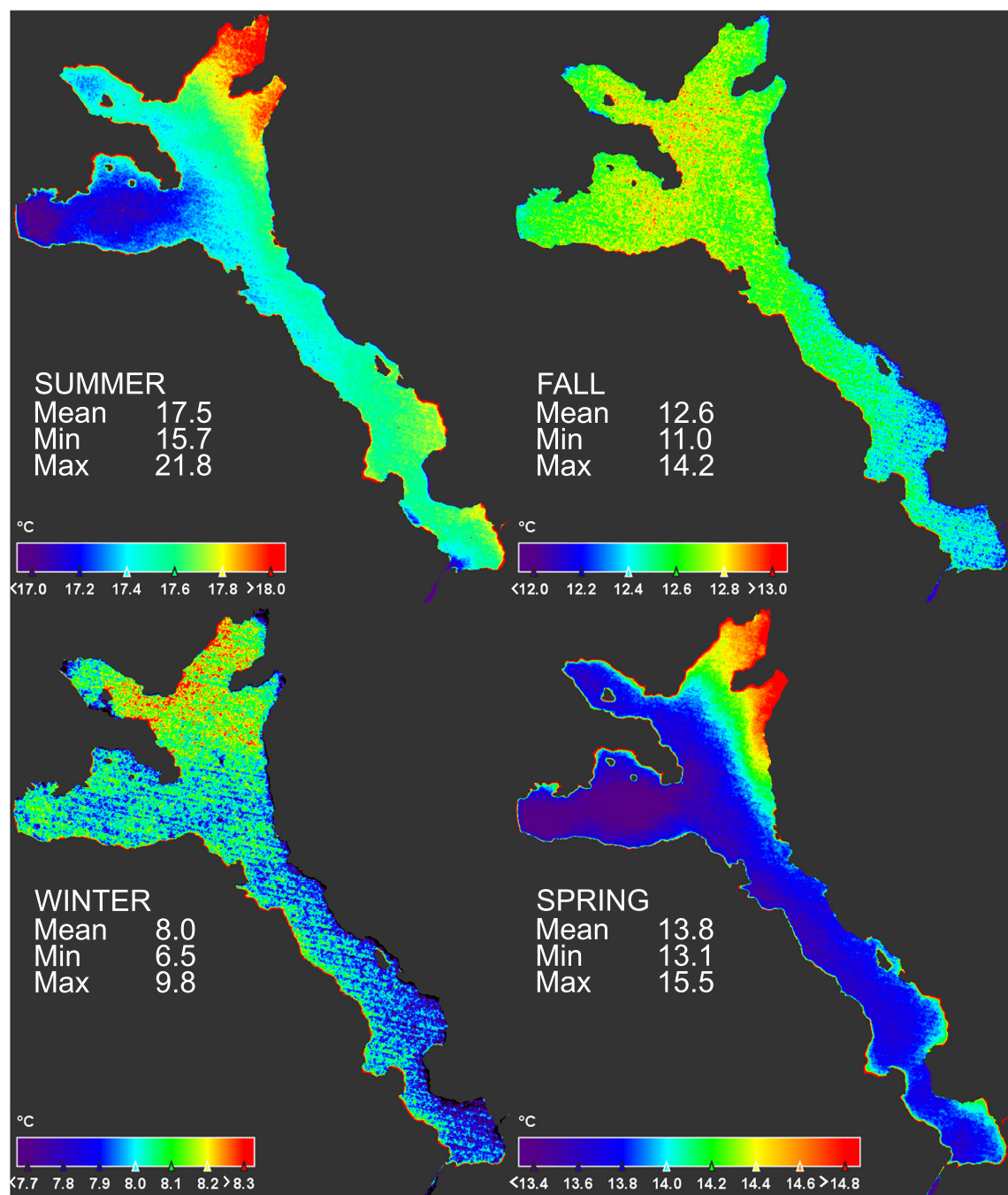


Fig. 4. Mean summer (January–March; $n = 29$ images), fall (April–June; $n = 6$), winter (July–September; $n = 10$) and spring (October–December; $n = 22$) surface water temperature of Lake Panguipulli during a period of 1998–2018 derived from Landsat 5/7/8 satellite images ($30 \times 30\text{ m}$ resolution) with clear sky conditions. Whole lake mean, minimum and maximum values are also given.

in spring and fall both field and satellite data showed wider variation and no significant differences (Fig. 3). Seasonal long-term means of turbidity from satellite imagery did not show significant differences from *in situ* data in any of the seasons. The range of minimum and maximum values was wide. In the case of chlorophyll *a*, spring and summer means from satellite were $0.5 \mu\text{g L}^{-1}$ higher than *in situ*. In fall and winter, no significant differences were observed (Fig. 3).

3.2. Seasonal variation of water characteristics

Satellite-derived data indicated strong seasonal variation of SWT, with whole lake averages ranging from 8.0°C in winter to 17.5°C in summer. In fall, the cooling to 12.6°C and in spring warming to 13.8°C was observed (Fig. 4). This seasonal pattern was confirmed with the analyses of the three sites (Table 4, see also Fig. 3). Based on the analysis of monthly variation from 1998 to 2018 data from the nine sites, SWT was at its lowest in July (mean $7.5\text{--}8.0^\circ\text{C}$ in sites 1–9) and August ($7.3\text{--}7.8^\circ\text{C}$), starting to warm from September ($8.2\text{--}9.0^\circ\text{C}$) onward. December ($16.4\text{--}17.5^\circ\text{C}$), January ($16.7\text{--}17.8^\circ\text{C}$), February ($17.6\text{--}18.2^\circ\text{C}$) and March ($16.9\text{--}17.2^\circ\text{C}$) presented the highest SWT. Higher inter-annual variation (SD) was observed in spring-summer due to higher number of analysed images (Fig. 5).

Satellite data showed lower whole lake mean turbidity in fall and summer ($1.3\text{--}1.6 \text{ FNU}$) than in spring and winter ($2.2\text{--}2.4 \text{ FNU}$) (Fig. 6). The lower turbidity in summer than in winter was significant in the analyses of the three sites (Table 4, see also Fig. 3). Based on the seasonal analyses of chlorophyll *a* from five sites, only the difference between lower summer ($1.1 \mu\text{g L}^{-1}$) and higher fall ($1.9 \mu\text{g L}^{-1}$) levels were significant (Table 4, see also Fig. 3).

3.3. Spatial variation of water characteristics

In spring (min-max $13.1\text{--}15.5^\circ\text{C}$), fall ($11.0\text{--}14.2^\circ\text{C}$) and winter ($6.5\text{--}9.8^\circ\text{C}$) the variation of SWT within the lake area was $2.4\text{--}3.3^\circ\text{C}$, while in summer spatial heterogeneity (6.1°C) was higher ($15.7\text{--}21.8^\circ\text{C}$). Spatial and seasonal patterns of SWT reflected the bathymetry and mixing patterns: warming of the shallow waters in spring extended to larger area along with summer stratification period, while mixing of the water column towards winter was reflected in spatially more homogenous SWT (Fig. 4).

The whole-lake mean chlorophyll *a* concentration for spring-summer period (2016–2017) was $1.1 \mu\text{g L}^{-1}$, ranging from 0.4 to $3.0 \mu\text{g L}^{-1}$. The highest concentrations were observed in the shallow bays, while deepest pelagic areas showing lowest levels (Fig. 7).

Based on a three-dimension plot, the nine study areas were clearly separated in summer according to the three studied parameters (Fig. 8). The deeper, central sites (especially the deepest point site 9; also sites 3, 4, 8) were separated from the bay areas (Huenehue Bay (site 7), Panguipulli Bay (sites 1–2), Choshuenco Bay (site 5)) by lower chlorophyll levels. Temperature further separated the central sites and even more clearly the bay sites from each other as groups. Deep Peligro Bay (site 6) and the southernmost site 5 (Choshuenco Bay) close to a river effluent were associated with higher turbidity and lower SWT. In winter, although a gradient of chlorophyll from lower levels in the central-southern sites (4–5, 8–9) to higher levels towards northern bay areas (site 1–3, 6–7) can be distinguished, the sites were not clearly separated due to a rather homogenous SWT and strong variation of turbidity within sites (Fig. 8). Overall, no significant relationship between the three variables could be observed for all sites: only in winter, SWT was significantly related with Chl *a* (Fig. 8).

In Huenehue Bay (site 7) SWT was above lake average during all the seasons, while the deep, pelagic site 4 was cooler than lake average throughout the year (Fig. 9). The deep site 6 (Peligro Bay) showed lowest SWT anomalies. Higher mean turbidity was associated with the shallow Panguipulli Bay (sites 1 and 2), deeper Peligro Bay (site 6) and the southernmost Choshuenco Bay (site 5), the latter, however, presenting

strong seasonal variation. Highest range of anomalies was observed in spring (min -0.55 , max 0.61). Highest chlorophyll levels were associated with shallow Panguipulli Bay sites 1, 2 and Huenehue Bay site 7. The lowest mean anomaly was observed in the site with the maximum depth of the lake (site 9) (Fig. 9).

4. Discussion

4.1. Application of remote sensing techniques in Lake Panguipulli

Landsat satellites have provided improved opportunities for obtaining larger temporal and spatial scale lake surface water temperature (LSWT) data due to their long-term continuity, thermal bands and relatively fine spatial resolution. Infrared sensors measure skin temperature, while *in situ* measurements below surface reach a deeper water layer. Therefore, when validating satellite-derived data with field measurements, somewhat lower SWT are often obtained for skin as compared to bulk temperature (Wilson et al., 2013). This was also observed in the present study with bias of -2.1°C and RMSD of 2.8°C between satellite and field measurements. Seasonal long-term means confirmed the approximately 2°C difference between skin and bulk temperature. These coincide with the standard errors or differences between Landsat SWT and *in situ* data reported in other studies ($1\text{--}3^\circ\text{C}$; Wukelic et al., 1989; Kay et al., 2005; Lamaro et al., 2013; Schaeffer et al., 2018). Due to the limited coincidence of satellite overpass with field monitoring dates, wider than commonly used ($\pm 3\text{-d}$) match-up window was used in the present study, which likely overestimates the error. In fact, average error has been shown to increase as time lapse between satellite overpass and *in situ* measurement becomes wider (Schaeffer et al., 2018). In a large validation of SWT from Landsat 5 and 7 for a variety of lakes and reservoirs in the United States, Schaeffer et al. (2018) found a mean absolute error (MAE) of 1.3°C (bias -0.98°C) in pixels in open water area, while closer to land mean error increased ($<180 \text{ m MAE } 4.8^\circ\text{C}$; bias 4.5°C). This was attributed to a signal from land in mixed pixels close to the shore. In Lake Panguipulli, pixel areas used for validation were all $>300 \text{ m}$ from the shore thus no contribution from land was involved. However, regarding the satellite imagery of the whole lake area, the presence of mixed pixels at the border of the water body mask area, and thus potential overestimation of SWT in some areas close to the shore cannot be ruled out. It should be pointed out, however, that in the shallow areas

Table 4

Results of one-way ANOVA for the seasonal differences in surface water temperature (SWT), turbidity and chlorophyll *a* (Chl) estimated from satellite imagery in Lake Panguipulli. The data correspond to 3×3 (SWT) or 10×10 (turbidity and Chl) pixel area around sites 1, 4, 5, and additionally sites 2 and 3 for Chl (corresponding to Fig. 3). Landsat-5-7-8 images of 1998–2018 (for SWT and turbidity) and Sentinel-2A-B images of 2016–2017 (for Chl) were used. Seasonal means (in parenthesis) followed by the same letter are not significantly different ($p > 0.05$) within each variable according to Tukey post-hoc test.

| Source | SS | D.F. | MS | F | p | Comparisons of means (Tukey test) |
|------------------|----------|------|----------|--------|--------|--|
| SWT | | | | | | |
| Intercept | 23,075.5 | 1 | 23,075.5 | 5138.3 | 0.0001 | Summer (17.5°C) c |
| Season | 2170.4 | 3 | 723.4 | 161.1 | 0.0001 | Fall (12.5°C) b |
| Error | 884.7 | 197 | 4.4 | | | Winter (7.9°C) a Spring (13.7°C) b |
| Turbidity | | | | | | |
| Intercept | 687.2 | 1 | 687.2 | 386.1 | 0.0001 | Summer (1.9°A) |
| Season | 18.0 | 3 | 6.0 | 3.3 | 0.0196 | Fall (1.8°A, B) |
| Error | 318.5 | 179 | 1.7 | | | Winter (2.6°B) Spring (2.4°A, B) |
| Chl | | | | | | |
| Intercept | 107.1 | 1 | 107.1 | 272.7 | 0.0001 | Summer (1.1°a) |
| Season | 3.9 | 3 | 1.3 | 3.3 | 0.0255 | Fall (1.9°b) |
| Error | 20.8 | 53 | 0.3 | | | Winter (1.5°a, b) Spring (1.4°a, b) |

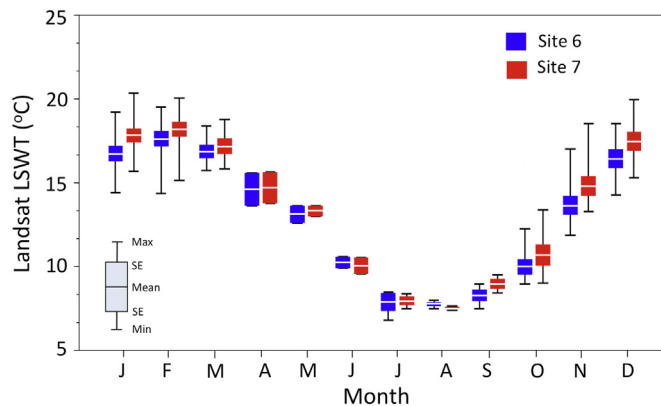


Fig. 5. Mean monthly surface water temperatures in two selected areas (3×3 pixel area) of Lake Panguipulli (Peligro Bay (site 6); Huenehue Bay (site 7); see Fig. 1) during a period of 1998–2018 derived from Landsat 5/7/8 satellite images (30 × 30 m resolution) with clear sky conditions. Mean \pm SD ($n = 7$ –11 for spring–summer, $n = 2$ –4 for fall–winter).

(Panguipulli and Huanehue Bay) the near-shore sites were not included within the water mask (due to the presence of emergent vegetation) thus the interference from land pixels should be limited. Although near-shore areas are important in water quality monitoring as they respond rapidly to changes and can serve as early warning system (Shanafied et al., 2010), they present challenges from methodological point of view in remote sensing. It should also be taken into consideration that *in situ* measurements are made in a single sampling point while satellite data represent wider area (in the present study 3×3 pixel array *i.e.* 90 × 90 m area). Several other aspects, such as time of daily measurements, wind and climatic conditions etc., which furthermore involve unpredictable spatio-temporal dimensions, can complicate the comparative analysis between field and satellite data (Wilson et al., 2013).

Seasonal long-term means of turbidity predicted from satellite imagery corresponded to those from *in situ* data. The used switching scheme algorithm has been shown to be suitable for a wide gradient (1–1000 FNU) of turbidity in coastal and estuarine waters, independent of particulate type or regional differences (Dogliotti et al., 2015). However, a need to further evaluate its sensitivity at lower turbidity range was indicated (Dogliotti et al., 2015). Therefore the very low minimum values

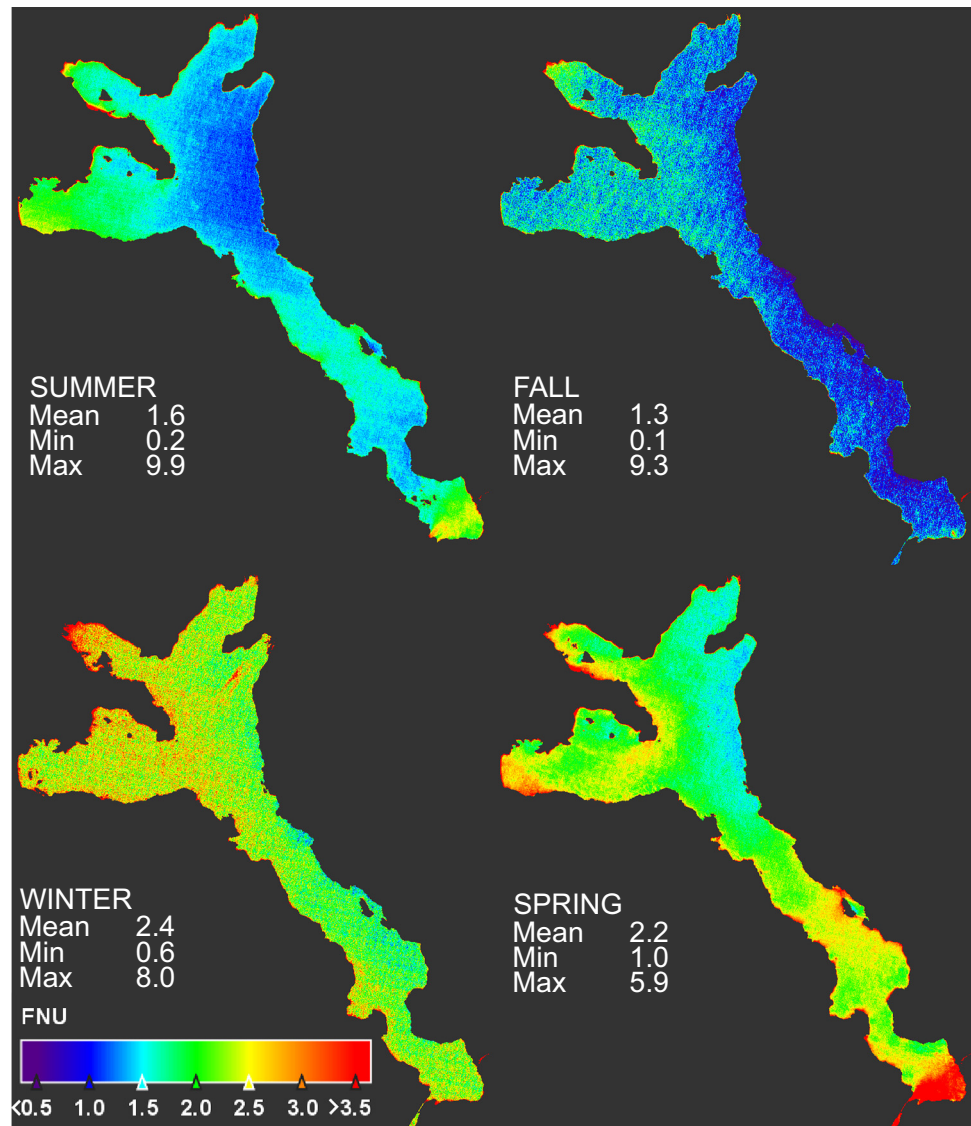


Fig. 6. Mean summer (January–March; $n = 27$ images), fall (April–June; $n = 7$), winter (July–September; $n = 10$) and spring (October–December; $n = 17$) turbidity of Lake Panguipulli during a period of 1998–2018 derived from Landsat 5/7/8 satellite images (30 × 30 m resolution) with clear sky conditions. Whole lake mean, minimum and maximum values are given.

predicted for Lake Panguipulli in summer-fall could be expected to present lower accuracy. Overall, the turbidity in this lake ranged 0.1–9.9 FNU (whole lake means of 1.3–2.4 FNU) showing strong variation, which made the observation of accurate seasonal trends less precise.

The predicted chlorophyll *a* concentrations from satellite imagery with the blue/green band ratio algorithm (OC2v2) of O'Reilly et al. (2000), originally the standard algorithm for estimations of global ocean chlorophyll distribution by NASA, were within the range of field observations, thus providing a reasonable accuracy. However, slight overestimation was observed in summer-spring (*i.e.* during the lowest chlorophyll periods), thus did not fully capture the seasonal variation. Likely reasons for this are the precision of the used algorithm to distinguish the differences at such low chlorophyll levels and interference from turbidity in the near-shore areas with river influence. This is in agreement with studies carried out in North American Great Lakes, showing that simple band ratio algorithms (two band (OC2) and four band (OC4)) provide reasonable estimates of chlorophyll amount not only in oceans but also in lakes, especially in their off-shore areas where interference from other optically active components (*e.g.* CDOM, particulate matter) is lower (reviewed by Lesht et al., 2012). Although there was a tendency of overestimation of low and underestimation of high chlorophyll concentrations, the temporal and spatial variations were found to coincide adequately with the field measurements (reviewed by Lesht et al., 2012), which was also observed in the present study. The optical complexity of lakes (with seasonal and spatial variation), their proximity to land, and continental atmosphere have been identified among the challenges for the retrieval of reliable parameters with wider applicability. Thus, validation of these

techniques accompanied by improved knowledge on the variability of different types of fresh waters is required (reviewed by Palmer et al., 2015; Dörnhöfer and Oppelt, 2016). Recently, Lesht et al. (2013) proposed a new single band ratio algorithm (based on the same OC4 band ratios) with sensor-specific coefficients, with improved application across lakes and seasons.

4.2. Seasonal and intra-lake variation of water properties

Although the frequency of the available Landsat imagery with suitable characteristics for the present study did not allow reliable evaluation of long-term trends, the results reinforce the importance of considering both the intra-lake and seasonal variation. Satellite-derived data allowed confirming the seasonal patterns previously described for Lake Panguipulli (Campos et al., 1981) with the lowest chlorophyll *a* levels and highest clarity (*i.e.* lowest turbidity) in summer, extending them into a whole-lake scale. Spatial and seasonal patterns of SWT reflected the bathymetry and previously described mixing patterns of this lake: warming of the shallow bays in spring extended to wider area along with summer stratification period, while mixing of the water column was reflected in spatially more homogenous SWT in fall-winter. Spatial heterogeneity of the lake surface water was strongest in summer clearly separating the different lake areas based on SWT, turbidity and chlorophyll *a*. Higher turbidity was associated with bay areas influenced by river input. The patterns of turbidity are in accordance with those observed by Shanafield et al. (2010) in Lake Tahoe, overall baseline levels being very low, but rising in winter and spring along with precipitation and increased runoff. Marked spatial

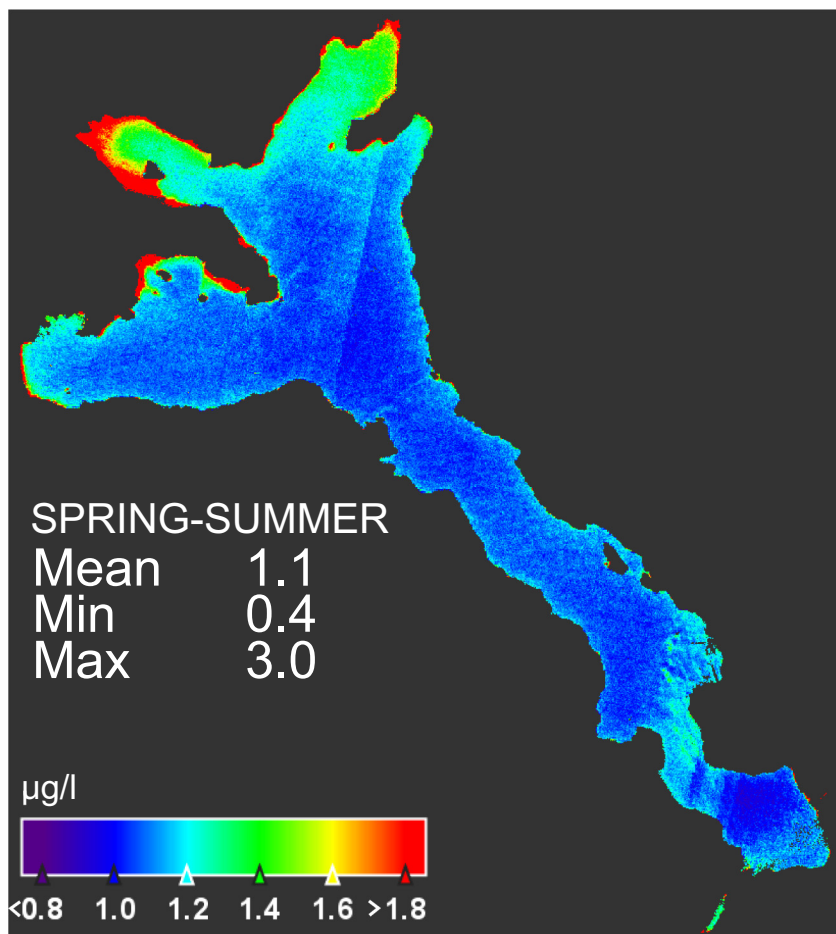


Fig. 7. Mean chlorophyll *a* concentration of Lake Panguipulli during spring-summer (November–March) 2016–2017 ($n = 6$ images) derived from Sentinel-2 satellite images (10 × 10 m resolution) with clear sky conditions. Whole lake mean, minimum and maximum values are given.

variation of water characteristics, as also reported e.g. for large humic lakes in eastern Finland, leads to a differential trophic status classification in different parts of a lake (Holopainen et al., 1993). Similar as in the present study, Bouffard et al. (2018) also found seasonally different correlations between chlorophyll *a* and temperature in Lake Geneva, which were associated with the up- and downwelling zones as a result of wind forcing.

According to a worldwide synthesis, summer surface temperatures in lakes have increased by 0.34 °C per decade from 1985 to 2009, being consistent with the global increase of air temperature (0.25 °C per decade), while cooling trend has been observed in 10% of the lakes (O'Reilly et al., 2015). However, trends were characterized by strong heterogeneity, depending on interactions of climate and geomorphic factors. Warming of near-surface temperatures has brought along stronger thermal stratification and steeper thermoclines (Kraemer et al., 2015; Richardson et al., 2017). Near-surface warming was observed in 80% and deep-water cooling in 50% of the studied North American lakes during 1975–2012 (Richardson et al., 2017). More transparent (Secchi depth >5 m) lakes showed faster surface warming and strengthening of thermal stratification. Thus, clear (e.g. high-altitude) lakes could be expected to show distinct warming trends than boreal lakes displaying contrasting water optics (e.g. Huovinen

and Goldman, 2000; Huovinen et al., 2003), which has been proposed as a characteristic applicable as an indicator of climate change (Williamson et al., 2014). In clear sub-alpine Lake Tahoe, long-term warming trend (1970–2002) has been observed both at the surface and 400 m (Coats et al., 2006). The reported deep water cooling trends in north Patagonian lakes, including Lake Panguipulli (Pizarro et al., 2016), are based on the rather limited (spatially and temporally) data from the monitoring database and thus might not represent fully the whole lake.

These reports point to a strong heterogeneity in the observed warming and cooling trends in lakes, influenced by interactions of climatic, geomorphic and local factors. Based on the results of the present study and other recent studies, it could be argued that the observed variability in the responses could be at least partly influenced by aspects related to study site and time. For example, trends in temperature based on single sampling point may not be representative of a whole lake as marked intra-lake heterogeneity has been reported, deep zones in large lakes showing overall faster warming rates (summer) (Woolway and Merchant, 2018; Woolway et al., 2016). This could be a result of the temporal persistence of anomalies associated with earlier onset of thermal stratification in these areas (Woolway and Merchant, 2018). In contrast, in small lakes summer near-surface temperatures can

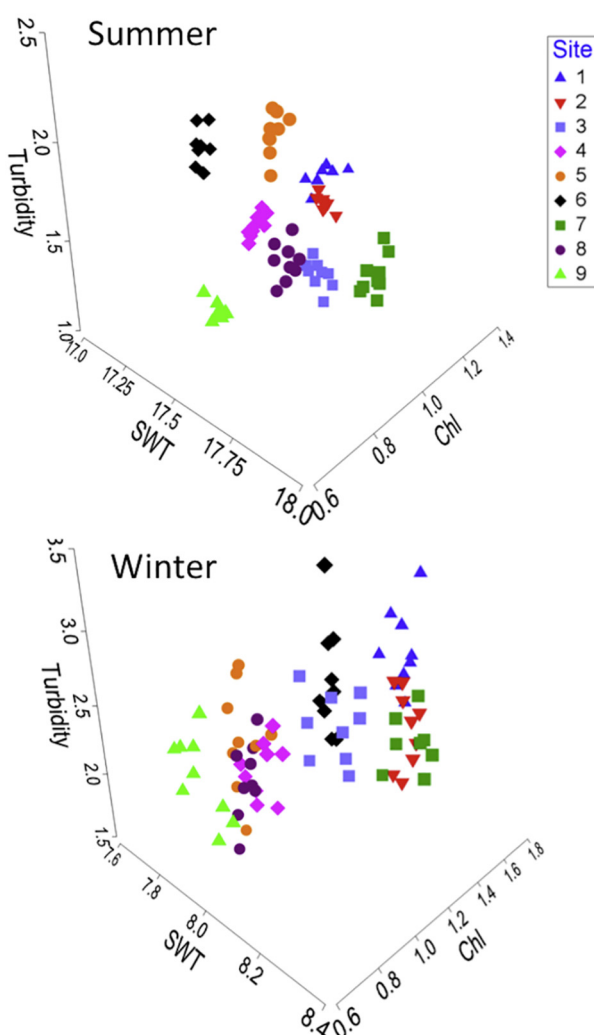


Fig. 8. Three-dimensional plot of the variability of satellite-derived surface water temperature (SWT), turbidity and chlorophyll *a* (Chl) of Lake Panguipulli associated with sites in summer and winter (left). Seasonal mean values of nine sites for a period of 1998–2018 for Landsat 5/7/8 satellite (SWT and turbidity) and 2016–2017 for Sentinel-2 (Chl) were used. For each site, data from nine pixels ($n = 9$) from 3×3 pixel area were used for SWT and turbidity. For Chl, 10×10 pixel area was divided into nine sub-areas ($n = 9$ values) for the analyses. Linear regression between the three parameters is also given (right).

display considerable daily variation, which can overlap the range of long-term change (Woolway et al., 2016). Many studies have focused on summer SWT warming rates, however, recently these trends have been shown to display seasonal variation (Winslow et al., 2017). Timing of warming trends will have important implications on those ecological processes that are specific to seasonal temperature signals, such as fish spawning (Winslow et al., 2017). In all, obtaining more detailed

information on spatial and temporal patterns of temperature is fundamental as it is a key parameter for most biological and chemical processes and needed for models e.g. forecasting harmful algal blooms (HABs; Schaeffer et al., 2018) or for explaining geographical expansion of invasive species (Adrian et al., 2009), also threatening north Patagonian lakes (Caputo et al., 2018). According to OECD (2016), expanding the coverage of water quality standards and implementation of

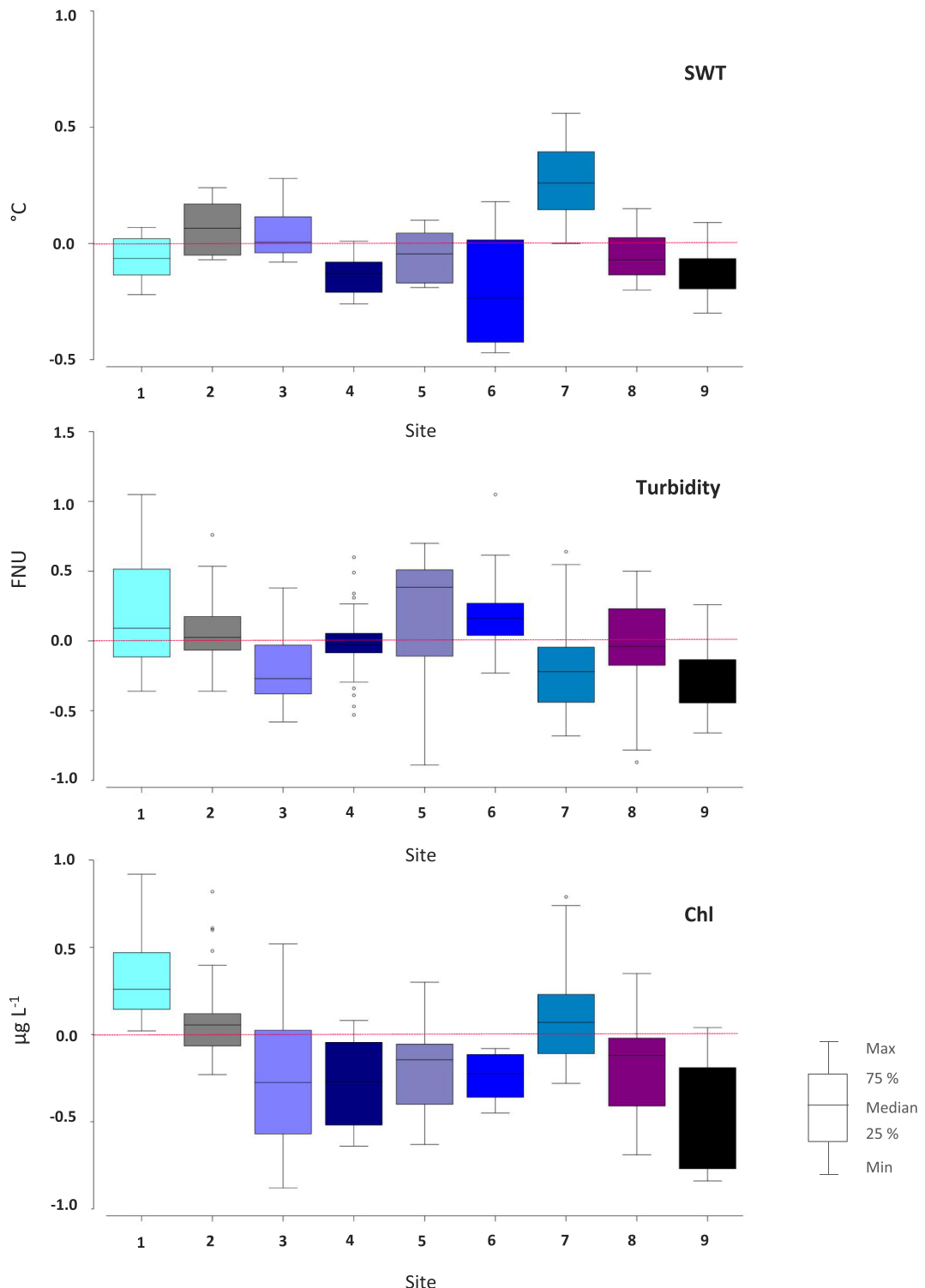


Fig. 9. Anomalies of satellite-derived surface water temperature (SWT), turbidity and chlorophyll *a* (chl) in different areas of Lake Panguipulli (sites 1–9) from the whole lake mean value. Mean values of all the seasons for a period of 1998–2018 for Landsat 5/7/8 satellite (SWT and turbidity) and 2016–2017 for Sentinel-2 (chlorophyll) were used. For each site, data from nine pixels ($n = 9$) from 3×3 pixel area were used for SWT and turbidity. For chlorophyll, 10×10 pixel area was divided into nine sub-areas ($n = 9$ values) for the analyses.

platforms for water quality, diversity and ecological information are recommended for lakes and rivers in Chile. In order to reinforce the application of the Secondary Environmental Quality Standards Quality (NSCA) for water quality of Chilean lakes, adopting remote sensing techniques, coupled with *in situ* limnological monitoring, would provide improved tools for diagnosis of the lake status and thus decision making to preserve aquatic ecosystems through maintenance or improvement of water quality.

4.3. Conclusions

Satellite-derived surface water temperature (SWT) showed good similarity with *in situ* data, difference (around 2 °C) being within the range of previous reports. Seasonal long-term means of turbidity predicted from satellite imagery corresponded to those from *in situ* data, while satellite-derived predictions of chlorophyll *a* (with OC2v2 algorithm) were somewhat less sensitive to detect seasonal variation due to a slight overestimation of the low chlorophyll levels of summer and spring. In near-shore areas, especially in the vicinity of river run-off, accuracy of satellite-derived chlorophyll prediction is likely influenced by turbidity.

Satellite-derived data allowed confirming the seasonal patterns of temperature and chlorophyll *a* previously described for Lake Panguipulli. SWT ranged from 8.0 °C (whole lake mean) in winter to 17.5 °C in summer, and chlorophyll *a* (1.1 mg L⁻¹) levels was at its lowest in summer. Also turbidity (1.6 FNU) was low in summer. Spatial patterns reflected the bathymetry and mixing patterns of this monomictic lake: warming of the shallow bays in spring extended to wider area along with summer stratification period, while mixing of the water column was reflected in spatially more homogenous SWT in fall-winter. Spatial heterogeneity was strongest in summer, clearly separating the different lake areas based on SWT, turbidity and chlorophyll *a*.

In all, mapping of spatial and temporal variation with satellite imagery allowed identifying lake areas with different characteristics and potential susceptibility to changes, thus improving our capacity of diagnosis of the lake status and strategies for water resource management.

Acknowledgments

The testing and application of remote sensing techniques was funded by Project FONDECYT 1161129 (to IG and PH). The Project Ventanilla Abierta UACH 2016 (to LC) allowed field monitoring of Lake Panguipulli in 2016.

The manuscript contains modified Copernicus Sentinel data [2016 and 2017]. Landsat and Sentinel data available from the U.S. Geological Survey.

References

- Adrian, R., O'Reilly, C.M., Zagarese, H., Baines, S.B., Hessen, D.O., et al., 2009. Lakes as sentinels of climate change. *Limnol. Oceanogr.* 54, 2283–2297.
- Baigún, C., Marinone, M.C., 1995. Cold-temperate lakes of South America: do they fit northern hemisphere models? *Arch. Hydrobiol.* 135, 23–51.
- Boisier, J.P., Rondanelli, R., Garreaud, R., Muñoz, F., 2016. Anthropogenic and natural contributions to the Southeast Pacific precipitation decline and recent megadrought in central Chile. *Geophys. Res. Lett.* 43, 413–421. <https://doi.org/10.1002/2015GL067265>.
- Bouffard, D., Kiefer, I., Wüest, A., Wunderle, S., Odermatt, D., 2018. Are surface temperature and chlorophyll in a large deep lake related? An analysis based on satellite observations in synergy with hydrodynamic modelling and *in-situ* data. *Rem. Sens. Environ.* 209, 510–523. <https://doi.org/10.1016/j.rse.2018.02.056>.
- Brown, F., Rivera, A., 2007. Climate changes and recent glacier behaviour in the Chilean Lake District. *Glob. Planet. Chang.* 59, 79–86.
- Bresciani, M., Vascellari, M., Giardino, C., Matta, E., 2012. Remote sensing supports the definition of the water quality status of Lake Omdeo (Italy). *Eur. J. Rem. Sens.* 45, 349–360. <https://doi.org/10.5721/EujRS20124530>.
- Bresciani, M., Cazzaniga, I., Astorini, M., Sforza, T., Buzzi, F., Morabito, G., Giardino, C., 2018. Mapping phytoplankton blooms in deep subalpine lakes from Sentinel-2A and Landsat-8. *Hydrobiologia* 824, 197–214. <https://doi.org/10.1007/s10750-017-3462-2>.
- Campos, H., Arenas, J., Steffen, W., Agüero, G., 1981. Morphometrical, physical and chemical limnology of Lake Panguipulli (Valdivia, Chile). *N. Jb. Geol. Paläont. Mh.* 10, 603–625.
- Caputo, L., Huovinen, P., Sommaruga, R., Gómez, I., 2018. Water transparency affects the survival of the medusa stage of the invasive freshwater jellyfish *Craspedacusta sowerbii*. *Hydrobiologia* 817, 179–191. <https://doi.org/10.1007/s10750-018-3520-4>.
- Coats, R., Perez-Losada, J., Schladow, G., Richards, R., Goldman, C., 2006. The warming of Lake Tahoe. *Clim. Chang.* 76, 121–148.
- Dirección General de Aguas (DGA), 2007. *Manual de normas y procedimientos del Departamento de Conservación y Protección de Recursos Hídricos*. SIT 132, 182.
- Dogliotti, A.J., Ruddick, K.G., Nechad, B., Doxaran, D., Knaeps, E., 2015. A single algorithm to retrieve turbidity from remotely-sensed data in all coastal and estuarine waters. *Rem. Sens. Env.* 156, 157–168. <https://doi.org/10.1016/j.rse.2014.09.020>.
- Dörnhöfer, K., Oppelt, N., 2016. Remote sensing for lake research and monitoring – recent advances. *Ecol. Indic.* 64, 105–122. <https://doi.org/10.1016/j.ecolind.2015.12.009>.
- Echeverría, C., Newton, A., Nahuelhual, L., Coomes, D., Rey-Benayas, J.M., 2012. How landscapes change: integration of spatial patterns and human processes in temperate landscapes of southern Chile. *Appl. Geogr.* 32, 822–831.
- Feyisa, G., Meilby, H., Fenner, R., Proud, S., 2014. Automated Water Extraction Index: a new technique for surface water mapping using Landsat imagery. *Rem. Sens. Env.* 140, 23–35. <https://doi.org/10.1016/j.rse.2013.08.029>.
- Giardino, C., Bresciani, M., Villa, P., Martinelli, A., 2010. Application of remote sensing in water management: the case study of Lake Trasimeno, Italy. *Water Res. Manage.* 24, 3885–3899. <https://doi.org/10.1007/s11269-010-9639-3>.
- Giardino, C., Bresciani, M., Stroppiana, D., Oggioni, A., Morabito, G., 2014. Optical remote sensing of lakes: an overview on Lake Maggiore. *J. Limnol.* 73, 201–214. <https://doi.org/10.4081/jlimnl.2014.817>.
- Hedin, L.O., Armesto, J.J., Johnson, A.H., 1995. Patterns of nutrient loss from unpolluted, old-growth temperate forests: evaluation of biogeochemical theory. *Ecology* 76, 493–509.
- Holopainen, A.-L., Huovinen, P., Huttunen, P., 1993. Horizontal distribution of phytoplankton in two large lakes in Eastern Finland. *Verh. Internat. Verein. Limnol.* 25, 557–562.
- Huovinen, P.S., Goldman, C.R., 2000. Inhibition of phytoplankton production by UV-B radiation in clear subalpine Lake Tahoe, California-Nevada. *Verh. Internat. Verein. Limnol.* 27, 157–160.
- Huovinen, P.S., Penttilä, H., Soimasuo, M.R., 2003. Spectral attenuation of solar ultraviolet radiation in humic lakes in Central Finland. *Chemosphere* 51, 205–214.
- Huovinen, P., Ramírez, J., Gómez, I., 2018. Remote sensing of albedo-reducing snow algae and impurities in the Maritime Antarctica. *ISPRS J. Photogram. Rem. Sens.* 146, 507–517.
- Huygens, D., Boeckx, P., Templer, P., Paulino, L., van Cleemput, O., Oyarzun, C., Müller, C., Godoy, R., 2008. Mechanisms for retention of bioavailable nitrogen in volcanic rainforest soils. *Nat. Geosci.* 1, 543–548.
- Jeffrey, S.W., Mantoura, R.F.C., Wright, S.W., 1997. Phytoplankton pigments in oceanography: guidelines to modern methods. *Monographs on Oceanographic Methodology*. vol. 10. UNESCO, Paris, France (661 pp).
- Kay, J.E., Kampf, S.K., Handcock, R.N., Cherkauer, K.A., Gillespie, A.R., Burges, S.J., 2005. Accuracy of lake and stream temperatures estimated from thermal infrared images. *J. Am. Water Res. Assoc.* 41, 1161–1175. <https://doi.org/10.1111/jawr.2005.41>.
- Kraemer, B.M., Anneville, O., Chandra, S., Dix, M., Kuusisto, E., et al., 2015. Morphometry and average temperature affect lake stratification responses to climate change. *Geophys. Res. Lett.* 42, 4981–4988. <https://doi.org/10.1002/2015GL064097>.
- Lamaro, A.A., Mariñelarena, A., Torrusio, S.E., Sala, S.E., 2013. Water surface temperature estimation from Landsat 7 ETM+ thermal infrared data using the generalized single-channel method: case study of Embalse del Rio Tercero (Cordoba, Argentina). *Adv. Space Res.* 51, 492–500. <https://doi.org/10.1016/j.asr.2012.09.032>.
- León-Muñoz, J., Echeverría, C., Marcé, R., Riss, W., Sherman, B., Iriarte, J.L., 2013. The combined impact of land use change and aquaculture on sediment and water quality in oligotrophic Lake Rupanco (North Patagonia, Chile, 40.8°S). *J. Environ. Manag.* 128, 283–291. <https://doi.org/10.1016/j.jenvman.2013.05.008>.
- Lesht, B.M., Barbiero, R.P., Warren, G.J., 2013. A bad-ratio algorithm for retrieving open-lake chlorophyll values from satellite observations of the Great Lakes. *J. Great Lakes Res.* 39, 138–152.
- Lesht, B.M., Barbiero, R.P., Warren, G.J., 2012. Satellite ocean color algorithms: a review of applications in the Great Lakes. *J. Great Lakes Res.* 38, 49–60. <https://doi.org/10.1016/j.jglr.2012.12.007>.
- Llames, M.E., Zagarese, H.E., 2009. Lakes and reservoirs of South America. In: Likens, Gene E. (Ed.), *Encyclopedia of Inland Waters*. vol. 2. Elsevier, Oxford, pp. 533–543.
- Modenutti, B.E., Balseiro, E.G., 2018. Preface: Andean Patagonian lakes as sensors of global change. *Hydrobiologia* 816, 1–2. <https://doi.org/10.1007/s10750-018-3622-z>.
- Myers, N., Mittermeier, R.A., Mittermeier, C.G., da Fonseca, G.A.B., Kent, J., 2000. Biodiversity hotspots for conservation priorities. *Nature* 403, 853–858.
- OECD, 2016. Biodiversity conservation and sustainable use. OECD Environmental Performance Reviews: Chile 2016. OECD Publishing, Paris <https://doi.org/10.1787/9789264252615-12-en>.
- O'Reilly, J.E., Maritorena, S., Mitchell, B.G., Siegel, D.A., Carder, K.L., Garver, S.A., Kahru, M., McClain, C., 1998. Ocean color chlorophyll algorithms for SeaWiFS. *J. Geophys. Res.* 103, 24,937–24,953.
- O'Reilly, J.E., Maritorena, S., Siegel, D.A., O'Brien, M.C., Toole, D., Mitchell, B.G., Kahru, M., Chavez, F.P., Strutton, P., Cota, G.F., Hooker, S.B., McClain, C.R., Carder, K.L., Müller-Karger, F., Harding, L., Magnuson, A., Phinney, D., Moore, G.F., Aiken, J., Arrigo, K.R., Letelier, R., Culver, M., 2000. Ocean Color Chlorophyll Algorithms for SeaWiFS, OC2 and OC4: Version 4. SeaWiFS Postlaunch Technical Report Series vol. 11. NASA Goddard Space Flight Center, Greenbelt, Maryland (Part 3, Ch. 2. NASA-TM-2000-206892).
- O'Reilly, C.M., Sharma, S., Gray, D.K., Hampton, S.E., Read, J.S., et al., 2015. Rapid and highly variable warming of lake surface waters around the globe. *Geophys. Res. Lett.* 42, 1–5. <https://doi.org/10.1002/2015GL066235>.

- Palmer, S.C.J., Kutser, T., Hunter, P.D., 2015. Remote sensing of inland waters: challenges, progress and future directions. *Rem. Sens. Env.* 157, 1–8. <https://doi.org/10.1016/j.rse.2014.09.021>.
- Perakis, S., Hedin, L.O., 2002. Nitrogen loss from unpolluted South American forests mainly via dissolved organic compounds. *Nature* 415, 416–419.
- Philipson, P., Kratzer, S., Mustapha, S.B., Strömbeck, N., Stelzer, K., 2016. Satellite-based water quality monitoring in Lake Vänern, Sweden. *Int. J. Rem. Sens.* 37, 3938–3960. <https://doi.org/10.1080/01431161.2016.1204480>.
- Pino, A., Cardyn, P., Grupo de Trabajo Panguipulli, 2014. *La reserva de la biosfera de los bosques templados lluviosos de los Andes australes y las singularidades territoriales de la comuna de Panguipulli*. In: Moreira-Muñoz, A., Borsdorf, A. (Eds.), *Reservas de la biosfera de Chile: Laboratorios para la sustentabilidad*. Academia de Ciencias Austríaca, Pontificia Universidad Católica de Chile, Instituto de Geografía, Santiago. Serie Geolibros vol. 17, pp. 190–207.
- Pizarro, J., Vergara, P.M., Rodríguez, J.A., Sanhueza, P.A., Castro, S.A., 2010. Nutrients dynamics in the main river basins of the centre-southern region of Chile. *J. Haz. Mat.* 175, 608–613.
- Pizarro, J., Vergara, P.M., Cerdá, S., Briones, D., 2016. Cooling and eutrophication of southern Chilean lakes. *Sci. Tot. Environ.* 541, 683–691. <https://doi.org/10.1016/j.scitotenv.2015.09.105>.
- Richardson, D.C., Melles, S.J., Pilla, R.M., Hetherington, A.L., Knoll, L.B., et al., 2017. Transparency, geomorphology and mixing regime explain variability in trends in lake temperature and stratification across northeastern North America (1975–2014). *Water* 9, 442. <https://doi.org/10.3390/w9060442>.
- Schaeffer, B.A., Schaeffer, K.G., Keith, D., Lunetta, R.S., Conmy, R., Gould, R.W., 2013. Barriers to adopting satellite remote sensing for water quality management. *Int. J. Rem. Sens.* 34 (21), 7534–7544. <https://doi.org/10.1080/01431161.2013.823524>.
- Schaeffer, B.A., James, J., Dwyer, J., Urquhart, E., Salls, W., Rover, J., Seegers, B., 2018. An initial validation of Landsat 5 and 7 derived surface water temperature for U.S. lakes, reservoirs, and estuaries. *Int. J. Rem. Sens.* <https://doi.org/10.1080/01431161.2018.1471545>.
- Shanafield, M.A., Susfalk, R.B., Taylor, K.C., 2010. Spatial and temporal patterns of near-shore clarity in Lake Tahoe from fine resolution turbidity measurements. *Lake Reserv. Manage.* 26, 178–184. <https://doi.org/10.1080/07438141.2010.504064>.
- Shimoda, Y., Azim, M.E., Perhar, G., Ramin, M., Kenney, M.A., et al., 2011. Our current understanding of lake ecosystem response to climate change: what have we really learned from north temperate deep lakes? *J. Great Lakes Res.* 37, 173–193. <https://doi.org/10.1016/j.jglr.2010.10.004>.
- Soto, D., 2002. Oligotrophic patterns in southern Chilean lakes: the relevance of nutrients and mixing depth. *Rev. Chil. Hist. Nat.* 75, 377–393.
- Steinhart, G.S., Likens, G.E., Soto, D., 2002. Physiological indicators of nutrient deficiency in phytoplankton in southern Chilean lakes. *Hydrobiologia* 489, 21–27.
- Toming, K., Kutser, T., Laas, A., Sepp, M., Paavel, B., Nõges, T., 2016. First experiences in mapping lake water quality parameters with Sentinel-2 MSI imagery. *Remote Sens.* 8, 640. <https://doi.org/10.3390/rs8080640>.
- Vanhellemont, Q., Ruddick, K., 2015. Remote sensing of environment advantages of high quality SWIR bands for ocean colour processing: examples from Landsat-8. *Rem. Sens. Env.* 161, 89–106. <https://doi.org/10.1016/j.rse.2015.02.007>.
- Williamson, C.E., Dodds, W., Kratz, T.K., Palmer, M.A., 2008. Lakes and streams as sentinels of environmental change in terrestrial and atmospheric processes. *Front. Ecol. Environ.* 6, 247–254. <https://doi.org/10.1890/070140>.
- Williamson, C.E., Saros, J.E., Schindler, D.W., 2009a. Sentinels of change. *Science* 323, 887–888. <https://doi.org/10.1126/science.1169443>.
- Williamson, C.E., Saros, J.E., Vincent, W.F., Smol, J.P., 2009b. Lakes and reservoirs as sentinels, integrators, and regulators of climate change. *Limnol. Oceanogr.* 54, 2273–2282.
- Williamson, C.E., Bretnrup, J.A., Zhang, J., Renwick, W.H., Hargreaves, B.R., et al., 2014. Lakes as sensors in the landscape: optical metrics as scalable sentinel responses to climate change. *Limnol. Oceanogr.* 59, 840–850.
- Wilson, R.C., Hook, S.J., Schneider, P., Schladow, S.G., 2013. Skin and bulk temperature difference at Lake Tahoe: a case study on lake skin effect. *J. Geophys. Res. Atmos.* 118, 10,332–10,346. <https://doi.org/10.1002/jgrd.50786>.
- Winslow, L.A., Read, J.S., Hansen, G.J.A., Rose, K.C., Robertson, D.M., 2017. Seasonality of change: summer warming rates do not fully represent effects of climate change on lake temperatures. *Limnol. Oceanogr.* 62, 2168–2178. <https://doi.org/10.1002/ln.10557>.
- Woolway, R.I., Merchant, C.J., 2018. Intralake heterogeneity of thermal responses to climate change: a study of large Northern Hemisphere lakes. *J. Geophys. Res.: Atm.* 123, 3087–3098. <https://doi.org/10.1002/2017JD027661>.
- Woolway, R.I., Jones, I.D., Maberly, S.C., French, J.R., Livingstone, D.M., Monteith, D.T., et al., 2016. Diel surface temperature range scales with lake size. *PLoS One* 11 (3), e0152466. <https://doi.org/10.1371/journal.pone.0152466>.
- Wukelic, G.E., Gibbons, D.E., Martucci, L.M., Foote, H.P., 1989. Radiometric calibration of Landsat Thematic Mapper thermal band. *Rem. Sens. Env.* 28, 339–347. [https://doi.org/10.1016/0034-4257\(89\)90125-9](https://doi.org/10.1016/0034-4257(89)90125-9).

Web references

- [dataset] Dirección General de Aguas, Ministerio de Obras Públicas, Gobierno de Chile, 2015. Base de datos calidad de agua (03_12_2014). <http://www.dga.cl/servicioshidrometeorologicos/> (accessed January 2019).
- <https://earthexplorer.usgs.gov/>.
- <http://step.esa.int/main/>.
- https://oceancolor.gsfc.nasa.gov/atbd/chlor_a/.
- <https://landsat.usgs.gov/landsat-8-l8-data-users-handbook-section-5>.
- <https://www.sernageomin.cl/red-nacional-de-vigilancia-volcanica/>.
- <http://odv.awi.de>.